Direct Spatial-temporal Observation of Barkhausen Avalanche in Low Dimensional Ferromagnetic System

Dong-Hyun Kim[a], Bosun Kang[a], Weilun Chao[a], Peter Fischer[a], Erik Anderson[a], Sug-Bong Choe[b], Mi-Young Im[c], and Sung-Chul Shin[c]

[a] Center for X-ray Optics, Lawrence Berkeley National Laboratory, Berkeley CA, USA;
[b] Department of Physics, Seoul National University, Seoul, Korea;
[c] Department of Physics, Korea Advanced Institute of Science and Technology, Daejeon, Korea

ABSTRACT

We report our direct observation of the Barkhausen avalanche in ferromagnetic thin film systems, where a collective spin behavior produces nontrivial fluctuations in magnetization change under an external magnetic field. For this study, we develop and use two direct full-field magnetic imaging techniques: magneto-optical microscope magnetometer (MOMM) and magnetic transmission X-ray microscopy (MTXM). From a direct visualization and a statistical analysis of the fluctuating domain images for Co thin films, we investigate the scaling behavior of the Barkhausen avalanche both on spatial and temporal scales using MOMM. We also investigate the reproducibility of the Barkhausen avalanche process. Interestingly, the partially stochastic nucleation behavior is observed for CoCrPt alloy films by means of MTXM on a nanometer scale comparable to the fundamental length scales such as the Barkhausen volume and the grain size of the polycrystalline films. Via these direct full-field observation techniques, dynamic details of Barkhausen avalanche are revealed.

Keywords: Barkhausen avalanche, magnetic domain, scaling behavior

1. INTRODUCTION

The magnetic domain dynamics in a ferromagnetic system has for long been a fundamental issue in magnetism. Formation and evolution of magnetic domain is a result of relevant energy minimization in collective spin behavior under a certain external magnetic field. When the domain is formed, each spin in the ferromagnetic system cannot behave independently and it shares its spin information with neighboring spins via exchange interaction, coupling with a lattice, and magnetostatic dipolar interaction. Therefore, macroscopic domain dynamics can be interpreted as a subsequent microscopic spin behavior. Any question related to the domain dynamics and to the magnetism is basically the question on how the domain wall moves and how the large number of spins behaves microscopically during the wall motion process.

Collective spin behavior on a submicron scale during the motion of domain wall has been investigated for the last decade by means of various experimental techniques,[1] motivated by the applications for magnetic information storage and magnetoelectric devices[2] as well as by the fundamental interest issued above. Much effort has been devoted to reveal the microscopic nature of spin behavior even down on an atomic scale during the domain wall motion. Very recently, it has been experimentally reported that the domain wall actually trapped between crystalline planes and it propagates by discrete jumps matching with the lattice periodicity.[3] And the effective mass of the single domain wall in its motion has been experimentally determined when it is coupled to the spin-polarized current.[4]

While the physical properties of domain wall have been intensively studied in microscopic details, little attention has been paid to the fundamental question on how the collective spin behavior will be affected when the moving domain wall meets disorders such as structural irregularities and defects inevitably distributed over the ferromagnetic system. Disorders generate pinning potentials and they usually pin the domain wall until the pinned wall is activated by the thermal fluctuation and released from being pinned. In this case, small amount

Further author information: (Send correspondence to Dong-Hyun Kim)
E-mail: dhkim@lbl.gov, Telephone: 1 510 486 5288

Fluctuations and Noise in Materials II, edited by Peter Svedlindh, Dragana Popovic, Michael B. Weissman, Proceedings of SPIE Vol. 5843 (SPIE, Bellingham, WA, 2005)
0277-786X/05/$15 · doi: 10.1117/12.609637

of local spin fluctuation may lead to totally different domain wall configurations over the entire ferromagnetic system.[5] One of the most beautiful features among these fluctuation-dominated phenomena is the critical scaling behavior, where the characteristic length disappears and the scale-free behavior appears. Specifically, if one measures the magnetization change induced by the domain wall movement under an external magnetic field, the measured magnetization change exhibits nontrivial fluctuation. Considering that the domain wall moves with a sequential jerky jumps in most of ferromagnetic systems, which is well known as the Barkhausen avalanche, the nontrivial fluctuation of intermittent magnetization change corresponds to each Barkhausen jump. It has been reported that the distribution of the Barkhausen jump size follows a power-law behavior and that the distribution can be fitted with a single value of the slope on log-log scale over several orders of magnitude, where the value of the slope allows us to determine the corresponding scaling exponent.[6,7] Interestingly, phenomena related to the moving domain wall through disordered medium via Barkhausen jumps have great number of analogies in wide variety of physical systems having any driven interface and correlated fluctuation,[8] such as surface growth, fluid invasion in porous media, dynamics of superconductor and superfluid, microfracture, and earthquakes.

So far, several models have been proposed to explain the scaling behavior of the Barkhausen effect. Classical criticality tuneable by amplitude and distribution of disorder was proposed by Sethna *et al.* within the context of a random-field Ising model.[9] On the other hand, self-organized criticality (SOC), achieved by self-organized evolution among barely stable states in a complex dynamic system was first introduced by Bak *et al.*[10] and then, applied to the Barkhausen avalanche by Cote and Meisel.[6] With an appropriate assumption of long-range dipolar interaction known to be essential in describing a ferromagnetic system,[7,11] Cizeau *et al.*[12,13] proposed a phenomenological model (CZDS) of domain wall dynamics in disordered system, which could explain more general situations than the previous models[14] and has been later investigated within more generalized scheme.[15]

From an experimental point of view, it should be noted that most experimental studies have been carried out on bulk samples using a classical inductive technique dated back to Barkhausen's pioneering work,[16] which is difficult to apply to low dimensional ferromagnetic system due to the low signal intensity. For this reason, very few experiments have been done on ferromagnetic thin films.[17] Only very recently, it has been reported that there exists a critical nature in ferromagnetic thin films by means of magnetooptical Kerr effect (MOKE)**?** and magnetic X-ray scattering,[19] where both techniques provide enough sensitivity even for the ferromagnetic thin film system, but still not sufficiently informative in describing real-space domain configuration. Based on MOKE measurement, the first reliable experiment reporting scaling behavior of Barkhausen effect has been carried out for Fe thin films,[18] although the experimental value of the scaling exponent is quite different from the values predicted by the existing models.[10,15,20] Magnetic X-ray scattering technique has been utilized to statistically investigate the correlation among repeated microscopic domain evolutions, where the statistical analysis has been carried for the scattered patterns in a momentum space, not in a real space.[19]

Clarification of the reason for this disagreement of the scaling exponent values and better understanding of the phenomenon require direct observation of the Barkhausen avalanche phenomenon in a real space. Direct visualization capability enables us to investigate the motion of domain wall in full details during the Barkhausen avalanche and offers a better understanding of this interesting physical phenomenon. In the present study, we report the use of novel magnetic imaging techniques for observation of domain wall fluctuation during the Barkhausen avalanche. We could directly visualize and analyze domain wall motions in various ferromagnetic films such as Co and CoCrPt by means of these full-field imaging techniques.

2. EXPERIMENT

We directly investigate domain wall motion in real time during the Barkhausen avalanche by means of a magnetooptical microscope magnetometer (MOMM), capable of time-resolved domain observation.[5,**?**] It basically consists of a polarizing optical microscope set to observe magnetic contrast via MOKE. The optical illumination path was tilted to provide an incident angle of 20^o from the film normal by shifting the position of the objective lens as well as adjusting the relevant optics. Therefore, we could visualize in-plane magnetic domains utilizing longitudinal MOKE. The spatial resolution is 2 μm and the Kerr angle resolution is 0.1^o in this setup. To store domain images, the system is equipped with advanced video processing having an image grabbing rate of 30 frames/s in real time. The time-resolved sequential domain images on a 400×320 μm^2 sample area were initially grabbed on a 256 gray scale and then, intensified by image processing technique such as background

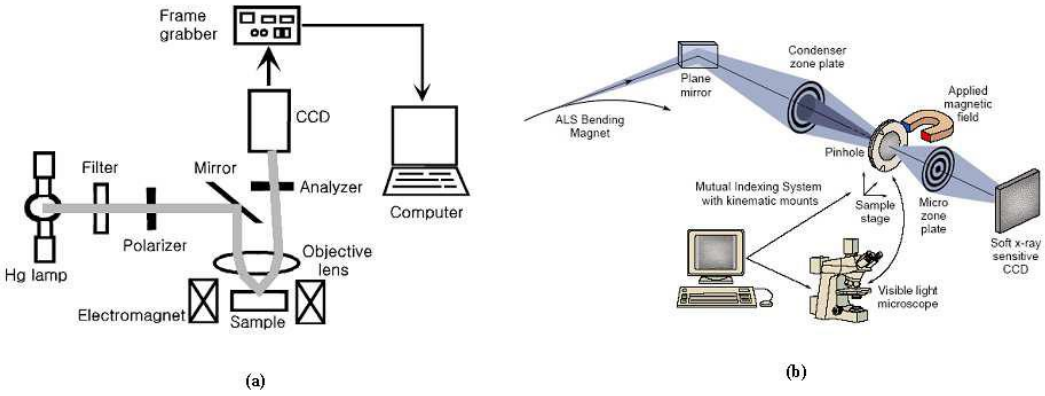

Figure 1. (a) Schematic diagram of MOMM setup. [Ref. 5] (b) Schematic diagram of XM-1 setup. [http://www.cxro.lbl.gov]

subtraction, noise filtering, and black-and-white image extraction. The Barkhausen avalanche was triggered by applying a constant magnetic field to an initially saturated sample. The strength of an applied field was about 99 % of the coercive field to eliminate the influence caused by the difference in the field-sweeping rates.[13] The Barkhausen jumps were directly visualized and characterized from serial time-resolved domain images. The schematic diagram of MOMM is illustrated in Fig. 1(a).

For additional understand of the scaling behavior of Barkhausen avalanche, extensions are needed for direct observations in both temporal and spatial dimensions. To this end, we are exploring the use an ultrahigh resolution full field magnetic transmission X-ray microscope (MTXM) developed by the Center for X-Ray Optics at beamline 6.1.2 in the Advanced Light Source Synchrotron, which uses XMCD contrast to enable us to observe the Barkhausen avalanche with full details on an ultra-fine spatial scale ($\sim$ 20 nm) and potentially, ultra-fast temporal scale ($\sim$70 ps).[22,23] To record the images, circularly polarized radiation passing through the ferromagnetic sample was projected through the micro zone plate onto a 2048×2048 pixel array of a CCD camera. Since the magnetic contrast is given by the projection of the magnetization onto the photon propagation direction, the CoCrPt sample with a perpendicular magnetic anisotropy was mounted with its surface normal parallel to the photon beam direction. To study the magnetization reversal in the CoCrPt films, the images have been recorded with varying external magnetic fields perpendicular to the film plane. The schematic diagram of MTXM is illustrated in Fig. 1(b).

We prepared several Co and CoCrPt films on glass substrates for MOMM study and membrane substrates for MTXM study by dc-magnetron sputtering. For simple Co films, an *in situ* magnetic field of 300 Oe was applied along a certain orientation in the film plane during deposition to induce magnetic anisotropy in this orientation, what was the same for all samples. Polycrystalline granular morphology with a cobalt grain size of a few tens of nanometers was confirmed by transmission electron microscopy (TEM). All the Co samples exhibit an in-plane magnetic anisotropy having uniaxial easy axis along the applied field orientation during the sample preparation.

For CoCrPt alloy films, 40-nm Ti buffer layer was first deposited on a 200-nm SiN membrane. The membrane substrate was used to allow sufficiently high transmittance of soft X-ray and thus, enough illumination intensity. All the CoCrPt alloy films exhibit a strong perpendicular magnetic anisotropy due to the good hcp(002) crystallographic alignment. The average grain size was determined from TEM images and was about several tens of nanometers.

3. RESULTS

3.1. Spatial fluctuation during Barkhausen avalanche

In Fig. 2(a), we illustrate a series of six representative domain-evolution patterns successively observed for 25-nm single Co film by means of the MOMM, where the colors code represents an elapsed time during 4 seconds

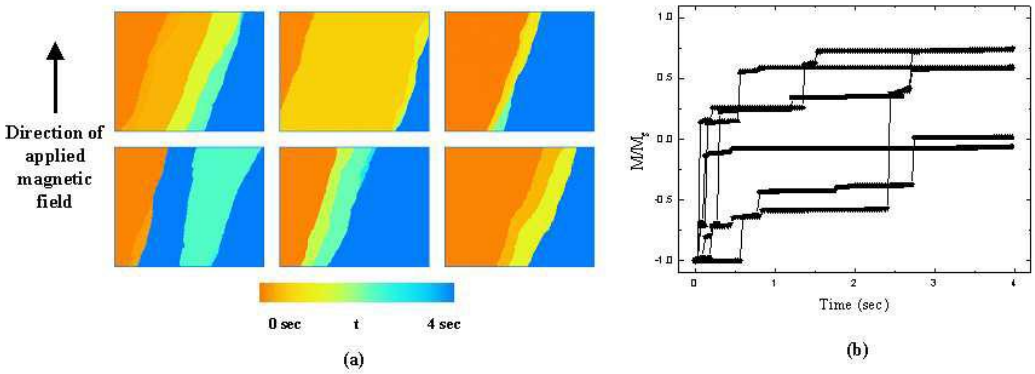

Figure 2. (a) A series of six domain images showing the avalanches of the domain structure captured successively on the same 400 × 320 μm^2 area of a 25-nm Co film. The color code represents the elapsed time from 0 to 4 seconds when magnetization reversal occurs. The sample was saturated downward first and then, a constant field was applied upward, denoted by the solid arrow. (b) Magnetization reversal curves obtained from the corresponding domain patterns of (a). [Ref. 5]

after applying an external field to trigger Barkhausen avalanche. Domain evolution patterns in each picture clearly exhibit typical avalanche-like features such as sudden and abrupt jumps during the reversal process. As we repeatedly carry out an observation at the same area keeping the same field of view, each magnetization reversal proceeds with quite different jumps with clearly different domain wall configuration. From the direct visualization, we conclude that the occurrence of each Barkhausen jump seems to be not reproducible with respect to interval, size, and location of the jump. And we can pinpoint the position of the domain wall in a real time and in a real space at each observation. Domains have a simple 180^o type walls throughout the avalanche process, which is expected from the uniaxial anisotropy induced during the sample preparation process. The observed avalanche-like characteristics prevails also for the other Co samples having different thickness of down to 5 nm.

Since we are dealing with digitized information of the time-resolved domain wall images captured at CCD, we can quantitatively determine the time-dependent magnetization reversal curve from the time-resolved domain image in Fig. 2(a). For ferromagnetic thin films having thickness comparable to the exchange length, we can assume that there is negligible change of spin direction along the thickness direction and the net magnetization parallel to an applied field direction is simply proportional to the reversed domain area. In Fig. 2(b), we plot the magnetization reversal curves corresponding to the six domain-evolution patterns in Fig. 2(a), where a stepwise feature is vividly witnessed. Each step in the curve corresponds to the area swept by a Barkhausen jump visualized in Fig. 2(a). The interesting characteristic of the curves in Fig. 2(b) is the presence of steps whose time interval and amplitude randomly fluctuate among the curves.

In our experiment, the Barkhausen jump size is determined from the direct measurement of abrupt areal change of real-time domain patterns observed using the MOMM, while all the other experiments up to now have determined the jump size via indirect methods such as inductive coil[7, 13, 14, 24] or MOKE technique.[18] Through a statistical analysis of the fluctuating size of Barkhausen jump from more than 1000 repetitive experiments for each sample, the distribution of Barkhausen jump size was obtained. In this analysis any Barkhausen jump which started or ended outside the observation area was not counted. In principle, counting only the jumps fully inside the frame provides us more reliable value of the scaling exponent.[25] However, most of domain walls have their two ends outside the field of view due to their uniaxial 180^o type domain wall structure. Number of images having the domain wall with both ends inside the field of view is less than one hundred, even though we have carried out more than several thousands of repeated observations. Practically, it is very difficult to achieve an enough number of statistical ensembles with images having both ends inside the field of view.

The distribution is found to exhibit a power law behavior and fitted as $P(s) \sim s^{-\tau}$ with scaling exponent

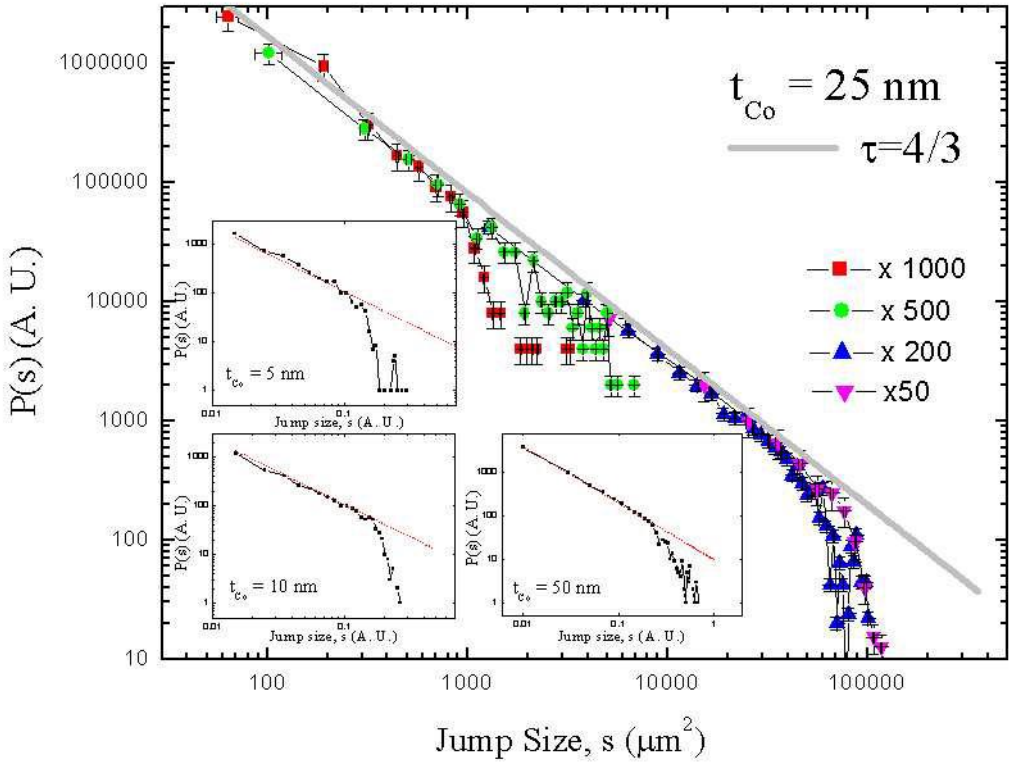

Figure 3. Distribution of Barkhausen jump size in 25-nm Co samples. Distributions in 5, 10, and 50-nm Co samples are shown in the insets. Fitting curve with (= 4/3 is denoted at each graph. [Ref. 5]

$\tau \sim 4/3$ as plotted in Fig. 3, where s is the Barkhausen jump size, normalized by the total area of observation. The most striking feature of Fig. 3 is the fact that the τ values are the same for both samples within the measurement error despite of the difference in their thickness. We may expect that the 50-nm film has about ten times number of defects compared with the 5-nm film, since two samples were prepared with the same preparation conditions except the thickness. Our experimental result implies an invariance of the scaling exponent τ irrespective of the number of defects in the Co thin films, within a thickness range comparable to the exchange length. This result reminds us the recent theoretical studies predicting that the variation of the number of defects does not affect the critical exponent, but only changes the cut-off of the power-law scaling in the distribution of the avalanche size.[8,20] However, the difference in the cut-off values of various Co films is not apparent enough to be quantitatively analyzed. The origin of the cut-off in scaling distribution is still controversial: the variation of disorder distribution,[8,20] the demagnetization effect,[13,24] or the finite size effect[6,10] has been suggested to explain the origin of the cut-off. The cut-off in Fig. 3 originated from the finite size effect since it accordingly varies with respect to the magnification and thus, with respect to the size of field of view.

Since the scaling exponent is the key parameter in description of the Barkhausen avalanche, we need to compare the value of τ with theoretical prediction. As discussed above, several models which adopt different assumptions and predict different values of scaling exponent, have been proposed. The prediction of τ for a two-dimensional system is diversely given as 1.5 for classical plain-old criticality,[20] ~1.0 for SOC.[10,26] Moreover, it is well known that difference may exist even among experimentally obtained scaling exponents due to different magnetization reversal mechanism, different domain type, or different driving field rate.[13,14,27] Therefore, before comparing the experimental and theoretical values it is necessary to carefully examine the assumptions of the models as well as to clearly define the experimental configurations by direct domain observation and driving-field

rate control.

We like to point out that the development of MOMM has opened a new possibility for direct full-field investigation of the Barkhausen avalanche phenomenon. However, the spatial resolution is limited by the diffraction limit of visible light ($\sim$ 400 nm). Very recently, spatial spin fluctuation during the Barkhausen avalanche has been investigated using magnetic force microscope (MFM) with significant improvement in spatial resolution.[28] Although a scanning microscope like MFM has an intrinsic disadvantage in studying fluctuation dominated avalanche-like behavior due to the tip-sample interaction, this technique with higher spatial resolution can be a meaningful complementary tool for this study.

3.2. Temporal fluctuation during Barkhausen avalanche

Barkhausen avalanche in ferromagnetic system is also known to exhibit a scaling behavior over wide range of temporal scale, during which the domain wall fluctuates nontrivially with intermittent avalanche-like bursts of magnetization jumps.[?] In addition to the jump size distribution, the distribution of the duration of each jump has been also known to follow a power-law behavior, providing another corresponding scaling exponent.[24,29] Interestingly, the statistical distributions of the spatiotemporally fluctuating quantities such as jump size and jump duration are often described based on universality. However, recent studies have been mainly devoted to investigate the spatial scaling behavior[5,18] and very little has been known about the temporal scaling behavior of the Barkhausen avalanche. It should be noted that the scaling behavior in spatial scale is closely related to that in temporal scale and they are not mutually independent.[13] Therefore, experimental observation and statistical analysis of Barkhausen avalanche in temporal scale as well as in spatial scale can extend our understanding of the scaling phenomenon.

In this section, we report a statistical analysis of the intermittency of Barkhausen avalanche by measuring the distribution of the separation time ΔT between adjacent two Barkhausen jumps in Co films having thickness ranging from 5 to 50 nm. The seperation time is determined from a direct time-resolved domain observation by means of MOMM.[30] The temporal resolution is about 30 ms and a series of 128 domain evolution patterns are captured sequentially during 4 seconds. The Barkhausen avalanche is triggered by applying a constant magnetic field to an initially saturated sample. The strength of an applied field is constant near the coercive field to eliminate the influence caused by the difference in the field-sweeping rates.[13,31] Intermittency of Barkhausen jumps are directly characterized and the seperation time ΔT is determined from serial time-resolved domain images. A series of 1000 measurements have been repeatedly carried out at 10 random positions of each sample to achieve reliable statistics.

The typical time-resolved domain evolution patterns and the scaling properties of jump size distribution have been intensively investigated in our previous section, where it has been revealed that discrete and sudden Barkhausen jumps with simple 180^o domain walls exist throughout the avalanche process. In the present section, we will focus on the intermittency of Barkhausen avalanche and its statistical distribution. In Fig. 4(a), we plot the magnetization reversal curve determined from a typical domain-evolution pattern observed at x200 magnification. From the magnetization curve we can easily determine when each jump has occurred and what the elapsed time separating two successive jumps is, as demonstrated in Fig. 4(a). All measurements for each sample are carried out during 4 seconds at x200 magnification. As the experiments are repeatedly performed at the same area of the film, magnetization reversal proceeds with quite different jumps every time as discussed in the previous section.

Through a statistical analysis of the fluctuating time interval ΔT between two Barkhausen jump events from more than 1000 times repetitive experiments for each sample, distribution of ΔT has been obtained. In determination of ΔT, there should be a threshold value in defining a jump event to identify the Barkhausen jump from the background noise. In our experimental configuration, the noise level is less than 1 % at x200 magnification and we only consider the Barkhausen jump event occurring with the measured jump size over than 1 % of the observed area (400×320 μm^2 at x200 magnification). In all samples, the distribution of ΔT determined in this way seems to have a power-law-like distribution, as illustrated in Fig. 4(b). The power-law form of the distribution does not vary with the slight change of threshold in counting jump events from 1 % to 2 %. Interestingly, one can notice that the four distribution curves from four kinds of samples having different thickness (5, 10, 25, and 50-nm) seem to fall in single universal curve within the measurement error. Unfortunately, the

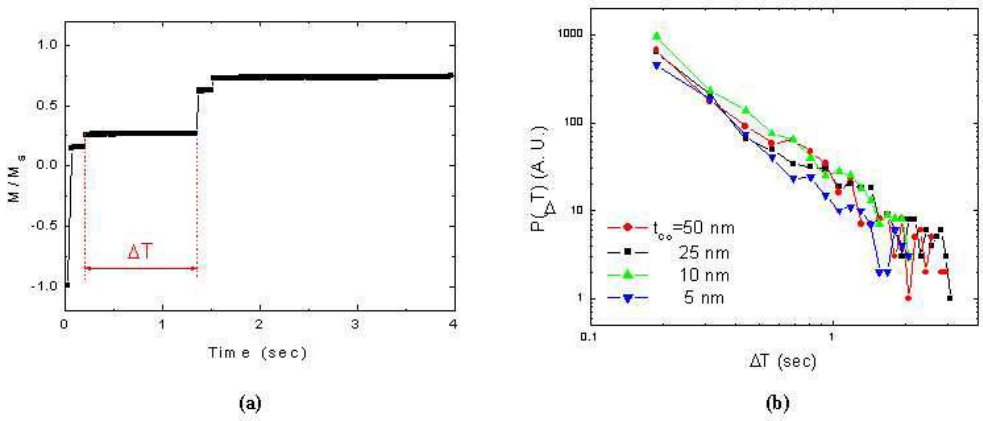

Figure 4. (a) Time-dependent magnetization reversal curve. (b) Distributions of ΔT which separates two adjacent Barkhausen jump events. [Ref. 30]

error is not negligible here and we believe the experimental proving of the universal intermittency behavior of Barkhausen avalanche is still an open problem. The relatively large error in case of the distribution of separation time compared to the case of the distribution of jump size seems to be originated from the smaller temporal measurement region ($0.2 \sim 4$ seconds). However, the exact reason is not clear, since even from the same set of time-resolved domain evolution patterns, the temporal fluctuation distribution has generally rough power-law form while the spatial fluctuation distribution has smoother power-law form. The temporal resolution of MOMM, in this work, is limited by 60 Hz frame grabbing and CCD operation time ($\sim$ 30 ms), which is not enough to fully investigate the fast dynamics of the Barkhausen avalanche. Development of faster observation technique is required for further in-depth study of temporal scaling behavior of the Barkhausen avalanche.

3.3. Reproducibility of Barkhausen avalanche

A visualization capability of the MOMM enables us to directly investigate the motion of domain wall in the Barkhausen avalanches. The repeated observation of the domain wall motion reveals that there exist some pinning segments around which domain walls are very flexible. The flexible part of domain wall moves forward via Barkhausen jump, while the pinned part is fixed at the same position for a relatively long time. This is quite expected because of the role of disorders as the pinning sites. It is very interesting to determine whether the domain wall fluctuation continues to appear even when a strong pinning site exists in the observed area. Time-resolved images of domain walls around the strong point-like pinning site were repeatedly obtained at the same area as illustrated in Fig. 5, where the position of point-like pinning site is indicated by the dashed arrow. As clearly seen in Fig. 5, the domain wall is still flexible in this case.

In Fig. 6, we provide another interesting example of critical fluctuation of Barkhausen avalanche in the case of a linear defect. From the time-resolved images illustrated in Fig. 3, we may expect that there exists a nearly horizontal linear defect, since all the domain evolution patterns indicate a common stop of evolution at linear line at the same location indicated by dotted line. Even in this extreme situation where the strong linear defect is expected to exist, the detailed propagation of domain wall shows significant fluctuation with constraint introduced by the linear defect. Barkhausen jump occurs still in a random critical way, keeping the system still at the criticality.

For a arbitrary region without any clear sign of pinning site, we repeat our observations at the same area with the same experimental conditions and visualize the microscopic behavior of fluctuating domain walls. By superimposing these fluctuating domain walls of each observation, we can generate the probability map to find domain wall at a certain position, which directly indicates how reproducible the avalanche process at a position will be. In Fig. 7(a), we demonstrate four representative images of time-resolved domain evolution patterns observed successively at the same area with identical experimental conditions. Note that domain evolution

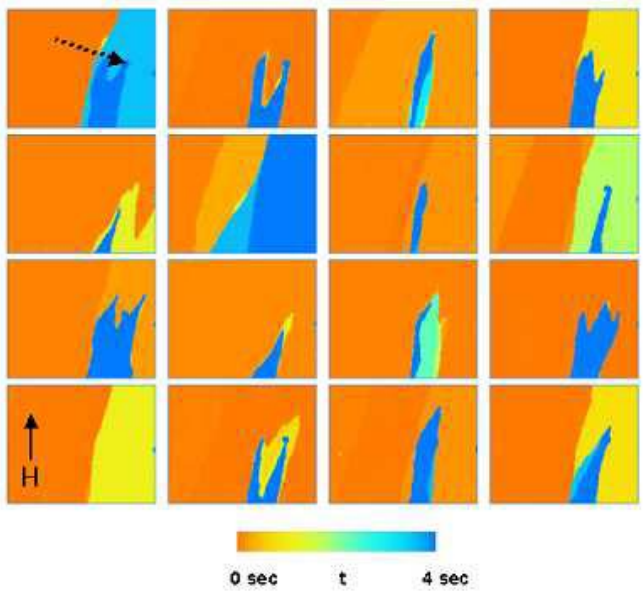

Figure 5. A series of domain evolution images captured repeatedly on the same 400x320 (m2 area with the same experimental conditions. The pinning site is indicated by the dotted arrow at the upper left image. The field is applied upwardly as denoted by solid arrow. [Ref. 32]

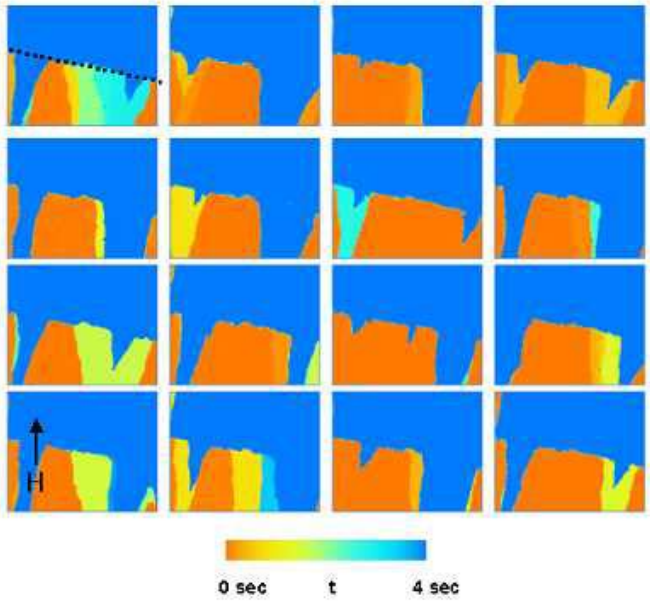

Figure 6. A series of domain evolution images captured repeatedly. The color code represents elapsed time. The dotted line at the upper left image indicates the estimated location of the linear defect. The field is applied upwardly. [Ref. 32]

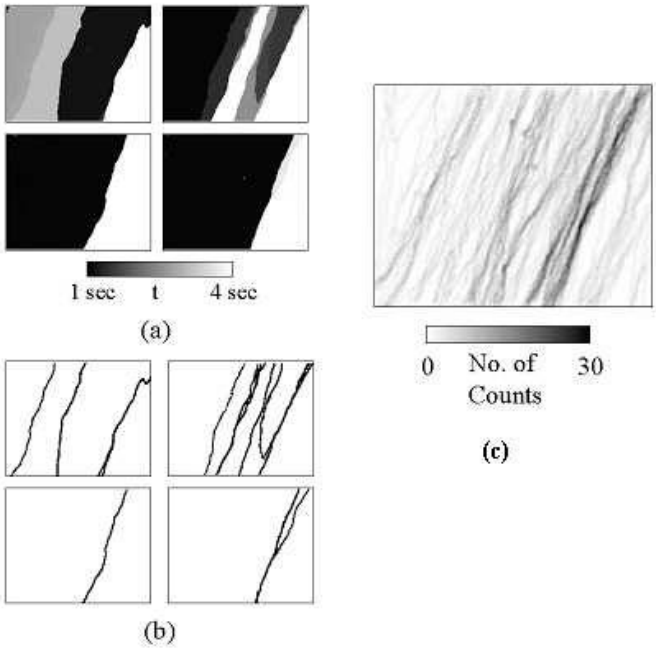

Figure 7. (a) Time-resolved domain patterns captured successively at the same area with identical experimental conditions. The sample magnetization was initially saturated downward and then, constant field was applied upward. (b) Domain walls determined via edge-finding image processing technique. (c) Probability map indicating spatial distribution of probability to find a domain wall at each position. Grey-level represents probability determined from 100 repeated observation. [Ref. 33]

patterns in each picture clearly exhibit discrete and sudden Barkhausen jumps and that domain configuration is not exactly reproducible at each observation. To quantitatively understand, we statistically analyze the domain wall configurations from our repeated observations. As a first step, we determine the domain-wall lines from the domain evolution patterns as illustrated in Fig. 7(b). The images of domain-wall lines in Fig. 7(b) are determined from the corresponding images of Fig. 7(a) via edge-finding image processing technique. For 100 repeated observations, we superimpose these images of domain-wall lines, where we can generate the probability map by counting how many times the domain wall is found at a certain position. Therefore, the map represents the spatial distribution of probability of finding domain wall at the position as vividly shown in Fig. 7(c). Interestingly enough, one can clearly notice that there exists a more probable region where the domain wall statistically prefers to exist.

However, question still remains on the reproducibility of avalanche process on a smaller scale, since the spatial resolution of MOMM is not enough to provide us any domain information of the Barkhausen avalanche on a submicron scale. For example, most of polycrystalline ferromagnetic films have smaller grain size about several tens of nanometers than the resolution of longitudinal MOMM ($\sim 2\ \mu m$) and no experimental study has been addressed to investigate the Barkhausen avalanche on a nanometer scale considering nanogranular structures. This grain volume is now comparable to the fundamental elementary unit volume in magnetization reversal mechanism with an assistance of thermal fluctuation, known as the Barkhausen volume. For investigation of the avalanche-like behavior on this fundamental length scale, magnetic imaging technique with better spatial resolution is required.

Recently, magnetization reversal behavior of CoCrPt alloy films has been investigated using MTXM developed by the Center for X-Ray Optics at beamline 6.1.2 in the Advanced Light Source Synchrotron.[34] MTXM basically uses X-ray magnetic circular dichroism (XMCD) contrast to enable us to observe domain dynamics with spatial

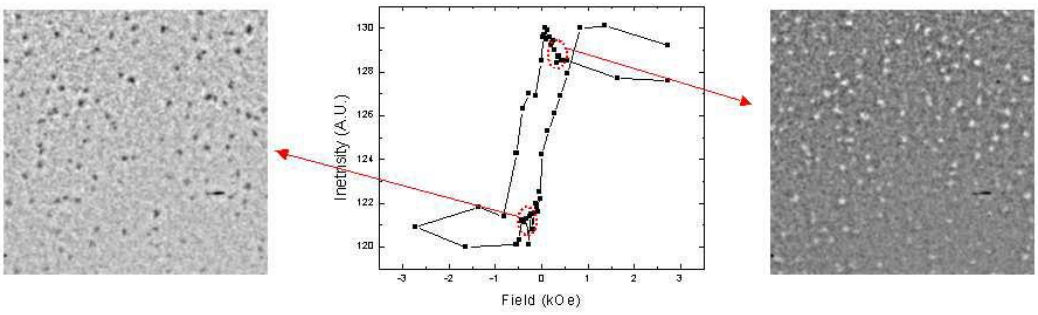

Figure 8. Typical nucleation dominant domain evolution image of CoCrPt alloy films and Hysteresis loop determined from quantitative analysis of XMCD contrast in field-dependent images.

resolution of $\sim$ 20 nm comparable to the grain size of most ferromagnetic polycrystalline films such as CoCrPt alloy films. Typical domain wall configuration of CoCrPt alloy films is shown in Figure 8. Unlike the case of an in-plane magnetic anisotropy sample having simple 180^o-type domain wall, reversed domains are first nucleated and then expanded by the wall motion.[35] Interestingly, the observed nucleation size is $\sim$ 80 nm or smaller, which is roughly corresponding to two grains of CoCrPt films or less. It is concluded that the nucleation starts with the reversal of individual grains in the sample.[34]

If we quantitatively analyze the field-dependent images, we can determine the magnetic hysteresis loop, as demonstrated in Fig. 8. If each grain is magnetically isolated and the thermal fluctuation of grain magnetization is negligible, the entire hysterectic magnetic cycles will be exactly reproducible since the energy landscape of the system is simply a sum of each grain contribution. In this case, the moving path of domain wall is predetermined and it finds its own path minimizing energy cost referring the fluctuation-tolerant energy landscape. However, the observed nucleation process in the present study seems to be at least partially stochastic, as depicted in Fig. 9. Many different nucleation sites appear, as we repeat our observation at the same experimental configuration, implying the possibility of intergranular magnetic interaction leading to the partially stochastic behavior in nucleation process. If we pay attention to the very recent experimental report on the Barkhausen avalanche using MFM, where it has been found that the scaling behavior exists in a wall expansion from the initially nucleated domain, not in a nucleation process,[28] it is considered that systematic study for clarifying an existence of the scaling behavior in nucleation process is required. To determine the origin of partial stochastic behavior of nucleation as demonstrated in Fig. 9, investigation with temperature-dependent and field-dependent magnetic imaging is essential to examine the statistical nature of thermal noise contributing to the magnetization reversal of nanogranular CoCrPt alloy films, which is being developed and integrated in MTXM.

4. CONCLUSIONS

We report our direct observation of the Barkhausen avalanche in ferromagnetic thin film systems. For this study we have used full-field magnetic imaging techniques: magneto-optical microscope magnetometer (MOMM) and magnetic transmission X-ray microscopy (MTXM). For example, by means of MOMM, we directly visualize and analyze domain wall fluctuation patterns in simple Co films, where a statistical analysis of the fluctuating size of Barkhausen jump from numerous repetitive observations has been carried out and the distribution of jump size is found to exhibit a universal power-law scaling behavior within the measurement error, irrespective of the film thickness ranging from 5 to 50 nm. On the other hand, we explore the use of an ultrahigh resolution full-field magnetic transmission X-ray microscope (MTXM) to visualize the Barkhausen avalanche process on nanometer scale comparable to the fundamental spatial scales such as Barkhausen volume and grain size of polycrystalline CoCrPt alloy films. Repeated observation using MTXM reveals that initial nucleation process is neither completely reproducible nor completely stochastic. Further investigation using MTXM is required to understand the underlying physical origin of the partially stochastic nucleation behavior on such a fundamental length scale.

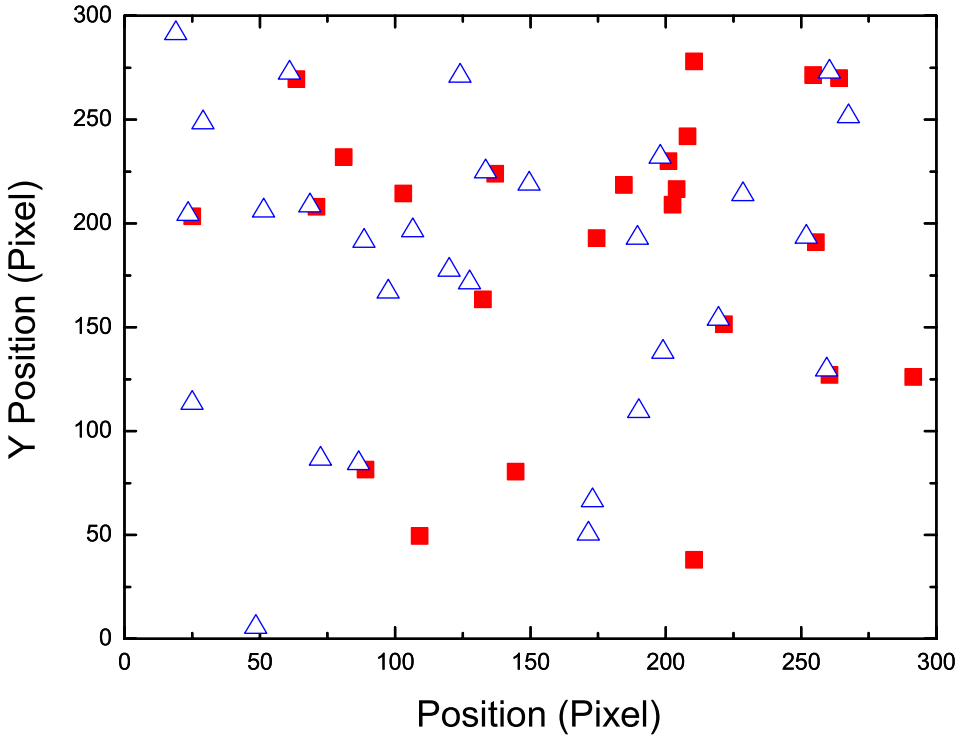

Figure 9. Coordinates of nucleation sites in two successive observations represented by red square and blue triangle.

ACKNOWLEDGMENTS

This work was supported by the Korea Research Foundation Grant (M01-2004-000-20348-0). This work was also supported by U.S. Department of Energy office of science under contract No. DE-AC03-76SF00098.

REFERENCES

1. S. A. Wolf, D. D. Awschalom, R. A. Buhrman, J. M. Daughton, S. von Molna'r, M. L. Roukes, A. Y. Chtchelkanova, and D. M. Treger, Science **294**, 1488 (2001).
2. P. Grünberg, Phys. Today. **54**, 31 (2001).
3. K. S. Novoselov, A. K. Geim, S. V. Dubonos, E. W. Hill, and I. V. Grigorieva, Nature **426**, 812 (2003).
4. E. Saitoh, H. Miyajima, T. Yamaoka, and G. Tatara, Nature **432**, 203 (2004).
5. D.-H. Kim, S.-B. Choe, and S.-C. Shin, Phys. Rev. Lett. **90**, 087203 (2003).
6. P. J. Cote and L. V. Meisel, Phys. Rev. Lett.
7. J. S. Urbach, R. C. Madison, and J. T. Markert, Phys. Rev. Lett. **75**, 276 (1995).
8. J. P. Sethna, K. A. Dahmen, and C. R. Myers, Nature **410**, 242(2001).
9. J. P. Sethna, K. Dahmen, S. Kartha, J. A. Krumshansl, B. W. Roberts, and J. D. Shore, Phys. Rev. Lett. **70**, 3347 (1993).
10. P. Bak, C. Tang, and K. Wiesenfeld, Phys. Rev. Lett. **59**, 381 (1987).
11. O. Narayan, Phys. Rev. Lett. **77**, 3855 (1996).
12. P. Cizeau, S. Zapperi, G. Durin, and H. E. Stanley, Phys. Rev. Lett. **79**, 4669 (1997).

13. S. Zapperi, P. Cizeau, G. Durin, and H. E. Stanley, Phys. Rev. B **58**, 6353 (1998).
14. B. Alessandro, C. Beatrice, G. Bertotti, and A. Montorsi, J. Appl. Phys. **68**, 2901 (1990); **68**, 2908 (1990)
15. A. Vázquez and O. Sotolongo-Costa, Phys. Rev. Lett. **84**, 1316 (2000).
16. H. Barkhausen, Z. Phys. **20**, 401 (1919).
17. N. J. Wiegman, Appl., Phys. **12**, 157 (1977); R. ter Stege and N. J. Wiegman, J. Phys. E. **11**, 791 (1978).
18. E. Puppin, Phys. Rev. Lett. **84**, 5415 (2000).
19. M. S. Pierce, R. G. Moore, L. B. Sorensen, S. D. Kevan, O. Hellwig, E. E. Fullerton, and J. B. Kortright, Phys. Rev. Lett. **90**, 175502 (2003).
20. O. Perković, K. Dahmen, and J. P. Sethna, Phys. Rev. Lett. **75**, 4528 (1995).
21. S.-B. Choe, D.-H. Kim, Y.-C. Cho, H.-J. Jang, K.-S. Ryu, H.-S. Lee, and S.-C. Shin, Rev. Sci. Instr., **73**, 2910 (2002).
22. P. Fischer, T. Eimüller, G. Schütz, G. Denbeaux, A. Pearson, L. Johnson, D. Attwood, S. Tsunashima, M. Kumazawa, N. Takagi, M. Köhler and G. Bayreuther, Rev. Sci. Instr., **72**, 2322 (2001).
23. H. Stoll, A. Puzic, B. van Waeyenberge, P. Fischer, J. Raabe, M. Buess, T. Haug, R. Höllinger, C. Back, D. Weiss, and G. Denbeaux, Appl. Phys. Lett. **84**, 3328 (2004).
24. G. Durin and S. Zapperi, Phys. Rev. Lett. **84**, 4705 (2000).
25. G. Durin and S. Zapperi, *The Science of Hysteresis*, edited by G. Bertotti and I. Mayergoyz.
26. F. Pázmandi, G. Zaránd, and G. T. Zimányi, Phys. Rev. Lett. **83**, 1034 (1999).
27. F. Pérez-Reche, B. Tadic, L. Mnosa, A Planes, and E. Vivies, Phys. Rev. Lett. **93**, 195701 (2004).
28. A. Schwarz and M. Liebmann, U. Kaiser, R. Wiesendanger, T. Noh, and D. Kim, Phys. Rev. Lett. **92**, 077206 (2004).
29. S. L. A. de Queiroz and M. Bahiana, Phys. Rev. E **64**, 66127 (2001).
30. D.-H. Kim and S.-C. Shin, J. Appl. Phys. **95**, 6971 (2004).
31. R. A. White and K. A. Dahmen, Phys. Rev. Lett. **91**, 85702 (2003).
32. D.-H. Kim, S.-B. Choe, and S.-C. Shin, J. Appl. Phys. **93**, 6564 (2003).
33. D.-H. Kim, S.-B. Choe, and S.-C. Shin, J. Mag. Mag. Mat. **272**, 720 (2004).
34. M.-Y. Im, P. Fischer, T. Eimüller, G. Denbeaux, S.-C. Shin, Appl. Phys. Lett. **83**, 4589 (2003).
35. S.-B. Choe and S.-C. Shin, Phys. Rev. Lett. **86**, 532 (2001).